

9 μ m Cutoff 128 \times 128 AlGaAs/ GaAs Quantum Well Infrared Photodetector Focal Plane Arrays*

Li Xianjie[†], Liu Yingbin, Feng Zhen, Guo Fan, Zhao Yonglin, Zhao Run, Zhou Rui, Lou Chen, and Zhang Shizu

(Hebei Semiconductor Research Institute, Shijiazhuang 050051, China)

Abstract: We design and fabricate a 128 \times 128 AlGaAs/ GaAs quantum well infrared photodetector focal plane array (FPA). The device is achieved by metal organic chemical vapor deposition and GaAs integrated circuit processing technology. A test structure of the photodetector with a mesa size of 300 μ m \times 300 μ m is also made in order to obtain the device parameters. The measured dark current density at 77 K is 1.5 $\times 10^{-3}$ A/cm² with a bias voltage of 2 V. The peak of the responsivity spectrum is at 8.4 μ m, with a cutoff wavelength of 9 μ m. The blackbody detectivity is shown to be 3.95 $\times 10^8$ (cm \cdot Hz^{1/2})/W. The final FPA is flip-chip bonded on a CMOS read-out integrated circuit. The infrared thermal images of some targets at room temperature background are successfully demonstrated at 80 K operating temperature with a ratio of dead pixels of less than 1 %.

Key words: AlGaAs/ GaAs; quantum well infrared photodetector; infrared thermal images

PACC: 7340L; 0762; 0260

CLC number: TN215

Document code: A

Article ID: 0253-4177(2006)08-1355-05

1 Introduction

AlGaAs/ GaAs quantum well infrared photodetectors (QWIPs), which are based on the advanced epitaxial material growth technology and the theory of energy band engineering, are becoming a focal point in the infrared photodetector focal plane array (FPA) field due to their excellent performance in response speed, pixel uniformity, radiation hardness, array format, fabrication cost, and multi-color integration. Thermal camera products with QWIP FPAs in 320 \times 240, 512 \times 486, 640 \times 512, and even 1024 \times 1024 pixel arrays have been developed successfully in some laboratories and companies for military and commercial applications, such as surveillance, reconnaissance, defense, astronomy, medicine, and industry^[1-9]. Pixelless QWIPs integrated with light emitting diodes (LEDs) have also been realized as an alternative approach to thermal imaging^[10]. Some results of single element QWIPs as well as thermal image demonstrations with a 128 \times 1 QWIP linear array and 64 \times 64 QWIP FPA have also been reported by

several groups in mainland China^[11-13]. Most of the above products and reports were obtained with molecular beam epitaxy (MBE) technology because of its accuracy and uniformity in the control of interface growth.

Considering the wide applicability of metal organic chemical vapor deposition (MOCVD) technology in the growth of multi-quantum well laser diode structures, we did many experiments in the growth of AlGaAs/ GaAs QWIPs with MOCVD. In this paper, we present the results of the epitaxial growth, design and fabrication of a long wavelength 128 \times 128 AlGaAs/ GaAs QWIP FPA with MOCVD technology. In addition, the infrared thermal images of some targets with a room temperature background are demonstrated with the 128 \times 128 AlGaAs/ GaAs QWIP flip-chip bonded on the related CMOS readout integrated circuit (ROIC) at 80 K operating temperature.

2 Epitaxial structure and growth

The epitaxial structure of the AlGaAs/ GaAs QWIP was grown on a commercially available

* Project supported by the Electronic Supporting Foundation (No. 41501070402)

[†] Corresponding author. Email: xianjie@tom.com

50mm semi-insulating GaAs (100) substrate with an Aixtron 2000 MOCVD system. Figure 1 shows a schematic of the AlGaAs/GaAs QWIP structure. The absorption layer is composed of n-doped AlGaAs/GaAs multi-quantum wells (MQWs) with 50 periods, each period of which consists of a 5nm well of GaAs (doped with Si to $n = 5 \times 10^{17} \text{cm}^{-3}$) and a 45nm barrier of $\text{Al}_{0.27}\text{Ga}_{0.73}\text{As}$. This photo-sensitive MQW structure is sandwiched between GaAs top and bottom contact layers doped by Si to $1.5 \times 10^{18} \text{cm}^{-3}$. The thicknesses of the top and bottom contact layers are 1000 and 1500nm, respectively. The parameter of the MQW and the index of Al are related to the peak wavelength of the responsivity spectrum and the transporting mode of the photoexcited carriers in the quantum wells.

| | | |
|-----------------------------------|--|-------|
| n ⁺ GaAs contact layer | 1μm, $1.5 \times 10^{18} \text{cm}^{-3}$ | } ×50 |
| AlGaAs barrier layer | 45nm | |
| GaAs well layer | 5nm, $5 \times 10^{17} \text{cm}^{-3}$ | |
| AlGaAs barrier layer | 45nm | |
| n ⁺ GaAs contact layer | 1.5μm, $1.5 \times 10^{18} \text{cm}^{-3}$ | |
| SI GaAs (100) substrate | | |

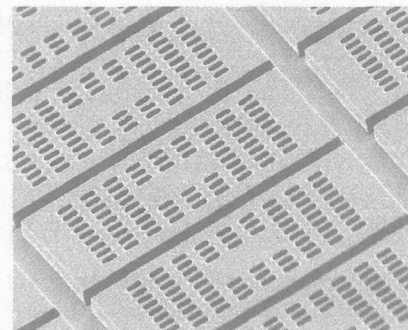
Fig. 1 Schematic diagram of AlGaAs/GaAs QWIP epitaxial structure

3 Device structure and fabrication process

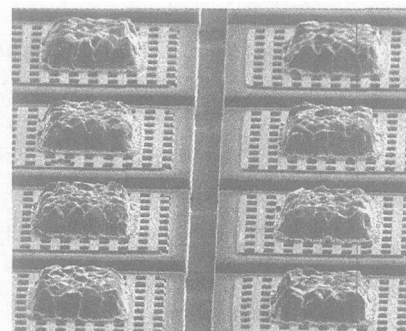
We have processed a test device with a mesa size of $300\mu\text{m} \times 300\mu\text{m}$ and a 128×128 -pixel QWIP FPA using the above epitaxial structure. In order to optimize the epitaxial parameters and the fabrication process of the final FPA, the test device was characterized to obtain the responsivity spectrum, dark current density, and detectivity. It is well known that the infrared radiation incident normal to the surface of the device is not absorbed by QWIPs unless the radiation has an electric field component normal to the layers of the superlattice^[6]. The test photodetector was coupled through a 45° polished facet on an edge of the device. For the FPA, a two-dimensional grating structure was designed and processed on the top of each pixel to couple the infrared light into the absorption layer of the QWIP. The grating structure consisted of a $2\mu\text{m} \times 2\mu\text{m}$ square cavity array with a center spac-

ing of $4\mu\text{m}$ and a depth of $0.75\mu\text{m}$. The 128×128 QWIP FPA with a pixel size of $45\mu\text{m} \times 45\mu\text{m}$ and a pitch of $50\mu\text{m}$ was realized using our in-house GaAs IC fabrication process. The chip size of the QWIP FPA was $6.9\text{mm} \times 6.9\text{mm}$.

The device process consists of standard photolithography, optical cavity grating etching, pixel mesa etching, and top and bottom ohmic contact formation. The optical grating and the pixel mesa were both formed by an inductively coupled plasma (ICP) dry etching process because of the highly lateral etching that occurs in wet chemical etching processes. The vertical, smooth sidewall of the mesa was obtained using Cl_2 and optimized process parameters. A standard multi-layer metal structure of AuGeNi/Au for n-type GaAs was evaporated, lifted-off, and annealed to form the top and bottom ohmic contacts. Finally, indium bumps were formed on the surface of the pixel elements, through which the QWIP FPA chip was flip-chip bonded on the related CMOS ROIC. Figure 2(a) is a scanning electronic microscope (SEM) photograph of the pixel elements with an ICP-etched optical cavity grat-



(a)



(b)

Fig. 2 SEM photographs of the pixels with ICP-etched optical cavity grating (a) and with indium bumps (b)

ing ,and Figure 2 (b) is a SEM photograph of the pixel elements with indium bumps.

4 Device performance of the test QWIP

The large area test QWIP photodetector was characterized using an on-wafer *I-V* analysis system consisting of Keithley 4200 semiconductor parameter analyzer and liquid nitrogen probe bench. Figure 3 shows the measured dark current density versus the bias voltage for the test device with a mesa size of 300μm ×300μm at 77 K with a room temperature background. The forward bias on the *x* axis means that the top contact of the device is forward biased. The dark current density is 1.5 × 10⁻³ and 5.5 × 10⁻⁴ A/cm² for applied bias voltages of +2 and -2V ,respectively. The asymmetry of the curve with forward bias and reverse bias in Fig. 3 is due to the asymmetry of the quantum well structure ,which is due to the distribution of Si dopant changing along the growth direction in the epitaxial process^[7,9].

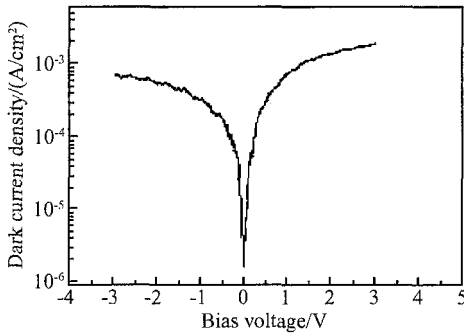


Fig. 3 Dark current density of test QWIP at 77 K versus the applied bias

In order to characterize the responsivity spectrum and the detectivity ,the test device with a 45° polished facet was bonded on an AlN carrier and then was mounted into a test dewar cooled by liquid nitrogen. Considering the temperature grades between the test QWIP ,the AlN carrier ,and the dewar ,the practical operating temperature of the QWIP was about 80 K instead of 77 K. Figure 4 is the responsivity spectrum of the test QWIP at a bias of 2V with a Nicolet 750 Fourier transform infrared (FTIR) spectrometer. The peak responsivity wavelength of the spectrum is at 8.4μm. The spectral width and the cutoff wavelength are λ_c =

20 % and λ_c = 9μm , respectively. This spectral width reveals that the type of intersubband transition for photoexcited electrons in the quantum wells may tend to the bound-to-continuum transition^[2,8].

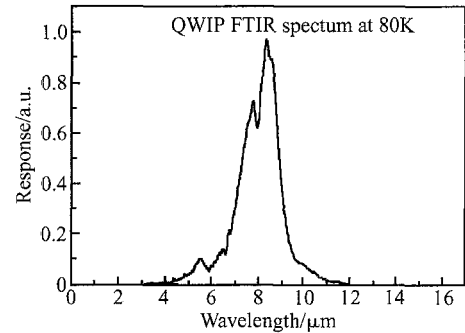


Fig. 4 Responsivity spectrum of the test QWIP at 80 K

The blackbody detectivity D_B^* is basically the signal-to-noise ratio of a radiation detector normalized to unit area and the operating bandwidth of the detector. Generally , D_B^* is defined as

$$D_B^* = R_B \frac{A f}{i_n} \tag{1}$$

where R_B is the blackbody responsivity , A is the area of the detector , f is the measurement bandwidth ,and i_n is the dark current noise. The blackbody detectivity was evaluated through a testing system with a calibrating blackbody source ,an optical chopper ,and a lock-in amplifier. The aperture diameter and the temperature of the blackbody were 15mm and 500 K , respectively. The distance between the blackbody window and the QWIP is 30cm. The radiation signal from the blackbody source was modulated by the chopper. The measured blackbody detectivity D_B^* was 3.95 × 10⁸ (cm · Hz^{1/2}) / W.

5 Thermal image result of the 128 × 128 QWIP FPA

A 128 ×128 CMOS ROIC was designed in our laboratory and fabricated using a commercially available 1.2μm CMOS process. The 128 × 128 QWIP FPA was flip-chip bonded on the related ROIC through indium bumps. In order to reduce the optical crosstalk between pixel elements ,the GaAs substrate of the QWIP FPA was then thinned and polished to about 100μm. The final QWIP FPA with ROIC was mounted into a dewar

with a germanium lens cooled by liquid nitride to demonstrate a thermal imaging camera. An image processing system was assembled to process the clock signals from the readout multiplexer and correct the obtained image. The thermal video images for static and moving targets in room temperature background were taken and demonstrated at a frame rate of 30 Hz on a monitor. The QWIP FPA realized excellent images with a ratio of dead pixels of less than 1%. Figures 5(a) and (b) are the thermal images at 80 K operating temperature after one-point correction for a man's face and a flame, respectively. The good image results for the $128 \times$

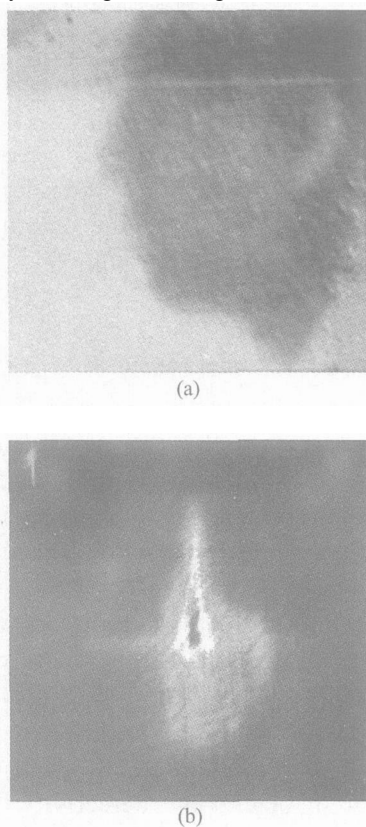


Fig. 5 Thermal images by 128×128 QWIP at 80 K operating temperature for a man's face (a) and a flame (b)

128 QWIP FPA reveal the advantages of the QWIP FPA in response speed and image uniformity. The image quality can be further improved by the following means. First, the epitaxial structure and process should be optimized to further lower the dark current and increase the detectivity; Second, the GaAs substrate of the QWIP should be thinned and polished to a thickness below $20 \mu\text{m}$ to eliminate more crosstalk between pixel elements; Third,

the QWIP operating temperature should be lowered below 65 K by using a Sterling cooler.

6 Conclusion

Using MOCVD technology and a GaAs integrated circuit fabrication process, we have designed and fabricated an n -doped large area testing AlGaAs/GaAs QWIP and a 128×128 AlGaAs/GaAs QWIP FPA. The measured dark current density of the test device was $1.5 \times 10^{-3} \text{ A/cm}^2$ at 77 K with an applied bias voltage of 2 V. The responsivity spectrum peaked at $8.4 \mu\text{m}$ and cutoff at $9 \mu\text{m}$; The blackbody detectivity D_B^* was shown to be $3.95 \times 10^8 (\text{cm} \cdot \text{Hz}^{1/2})/\text{W}$. The infrared thermal images of the targets at room temperature background were demonstrated with the 128×128 AlGaAs/GaAs QWIP FPA flip-chip bonded on the related CMOS readout integrated circuit at 80 K. The ratio of dead pixels was less than 1%, which shows the high yield of GaAs-based QWIP FPAs. These results also reveal that MOCVD technology is very promising in the application of QWIP epitaxial structure. A practical, large-format QWIP FPA will be demonstrated if the epitaxial structure, growth parameters, and fabrication process are optimized further.

Acknowledgements The authors would like to thank Prof. Zhang Yanbing and Engineer Hu Xiaoyan with North China Institute of Optoelectronic Technology and Prof. Zhang Yonggang with Shanghai Institute of Micro-system and Information of the CAS for their help in the measurement of detectivity and response spectrum.

References

- [1] Levine B F. Quantum-well infrared photodetectors. *J Appl Phys*, 1993, 74 (8) : R1
- [2] Levine B F, Zussman A, Kuo J M, et al. $19 \mu\text{m}$ cutoff long wavelength GaAs/Al_xGa_{1-x}As quantum well infrared photodetectors. *J Appl Phys*, 1992, 71 (10) : 5130
- [3] Liu H C, Wasilewski Z R, Buchanan M, et al. Segregation of Si doping in GaAs/AlGaAs quantum well and the cause of the asymmetry in the current voltage characteristics of intersubband infrared detector. *Appl Phys Lett*, 1993, 63 (6) : 761
- [4] Gunapala S D, Liu J K, Park J S, et al. $9 \mu\text{m}$ cutoff 256×256 GaAs/Al_xGa_{1-x}As quantum well infrared photodetector hand-held camera. *IEEE Trans Electron Devices*, 1997, 44: 51
- [5] Gunapala S D, Bandara S V, Singh A, et al. 640×486 long-

- wavelength two-color GaAs/ AlGaAs quantum well infrared photodetector (QWIP) focal plane array camera. IEEE Trans Electron Devices, 2000, 47: 963
- [6] Gunapala S D, Bandara S V, Liu J K, et al. 1024×1024 mid-wavelength and long-wavelength QWIP focal plane arrays for imaging applications. Semiconductor Science and Technology, 2005, 20: 473
- [7] Zussman A, Levine B F, Kuo J M, et al. Extended long-wavelength $\lambda = 11 \sim 15\mu\text{m}$ GaAs/ $\text{Al}_x\text{Ga}_{1-x}\text{As}$ quantum well infrared photodetectors. J Appl Phys, 1991, 70(9): 5101
- [8] Gunapala S D, Bandara S V. Quantum well infrared photodetector (QWIP) focal plane arrays. In: Semiconductors and semimetals. Academic Press, 1999, 62: 197
- [9] Liu H C, Wasilewski Z R, Buchanan M. Segregation of Si doping in GaAs/ $\text{Al}_x\text{Ga}_{1-x}\text{As}$ quantum wells and the cause of the asymmetry in the current-voltage characteristics. Appl Phys Lett, 1993, 63: 761
- [10] Liu H C, Dupont E, Byloos M, et al. QWIP-LED pixelless thermal imaging device. Inter J High Speed Electronics and Systems, 2002, 12(3): 891
- [11] Cai Weiyang, Li Zhifeng, Li Ning, et al. Photoluminescence characterization in GaAs/ AlGaAs quantum well infrared photodetectors. J Infrared Millim Waves, 2001, 20(1): 66 (in Chinese) [蔡炜颖, 李志锋, 李宁, 等. GaAs/ AlGaAs 量子阱红外探测器的光荧光表征. 红外与毫米波学报, 2001, 20(1): 66]
- [12] Yu Xiaozhong, Guo Xiandong. A 128×1 multi-quantum well infrared linear array and its signal readout. Infrared Technology, 1999, 241(2): 35 (in Chinese) [余晓中, 郭献东. 一种 128×1 的 AlGaAsGaAs 多量子阱红外探测器线阵及其信号的读出. 红外技术, 1999, 241(2): 35]
- [13] Li Ning, Li Na, Lu Wei, et al. Development of 64×64 pixel GaAs/ AlGaAs quantum well infrared photodetector focal plane array. J Infrared Millim Waves, 1999, 18(6): 427 (in Chinese) [李宁, 李娜, 陆卫, 等. 64×64 元 GaAs/ AlGaAs 多量子阱长波红外焦平面研制. 红外与毫米波学报, 1999, 18(6): 427]

$9\mu\text{m}$ 截止波长 128×128 AlGaAs/ GaAs 量子阱红外焦平面探测器阵列*

李献杰[†] 刘英斌 冯震 过帆 赵永林 赵润 周瑞 娄辰 张世祖

(河北半导体研究所, 石家庄 050051)

摘要: 报道了 128×128 AlGaAs/ GaAs 量子阱红外焦平面探测器阵列的设计和制作. 采用金属有机化学气相淀积外延技术生长外延材料, 并在 GaAs 集成电路工艺线上完成工艺制作. 为得到器件参数, 设计制作了台面尺寸为 $300\mu\text{m} \times 300\mu\text{m}$ 的大面积测试器件; 77K 下 2V 偏压时暗电流密度为 $1.5 \times 10^{-3}\text{A}/\text{cm}^2$; 80K 工作温度下, 器件峰值响应波长为 $8.4\mu\text{m}$, 截止波长为 $9\mu\text{m}$, 黑体探测率 D_B^* 为 $3.95 \times 10^8 (\text{cm} \cdot \text{Hz}^{1/2})/\text{W}$. 将 128×128 元 AlGaAs/ GaAs 量子阱红外焦平面探测器阵列芯片与相关 CMOS 读出电路芯片倒装焊互连, 在 80K 工作温度下实现了室温环境目标的红外热成像, 盲元率小于 1% .

关键词: AlGaAs/ GaAs; 量子阱红外探测器; 红外热成像

PACC: 7340L; 0762; 0260

中图分类号: TN215

文献标识码: A

文章编号: 0253-4177(2006)08-1355-05

* 电子支撑基金资助项目(批准号: 41501070402)

[†] 通信作者. Email: xianjie@tom.com

2006-02-05 收到, 2006-03-31 定稿